

Kent Academic Repository

Full text document (pdf)

Citation for published version

Videira, Marco A. M. and Lobo, Susana A. L. and Silva, Liliana S. O. and Palmer, David and Warren, Martin J. and Prieto, Manuel and Coutinho, Ana and Sousa, Filipa L. and Fernandes, Fábio and Saraiva, Lígia M. (2018) Staphylococcus aureus haem biosynthesis and acquisition pathways are linked through haem monooxygenase IsdG. *Molecular Microbiology*, 109 (3).

DOI

<https://doi.org/10.1111/mmi.14060>

Link to record in KAR

<https://kar.kent.ac.uk/68840/>

Document Version

Author's Accepted Manuscript

Copyright & reuse

Content in the Kent Academic Repository is made available for research purposes. Unless otherwise stated all content is protected by copyright and in the absence of an open licence (eg Creative Commons), permissions for further reuse of content should be sought from the publisher, author or other copyright holder.

Versions of research

The version in the Kent Academic Repository may differ from the final published version.

Users are advised to check <http://kar.kent.ac.uk> for the status of the paper. **Users should always cite the published version of record.**

Enquiries

For any further enquiries regarding the licence status of this document, please contact:

researchsupport@kent.ac.uk

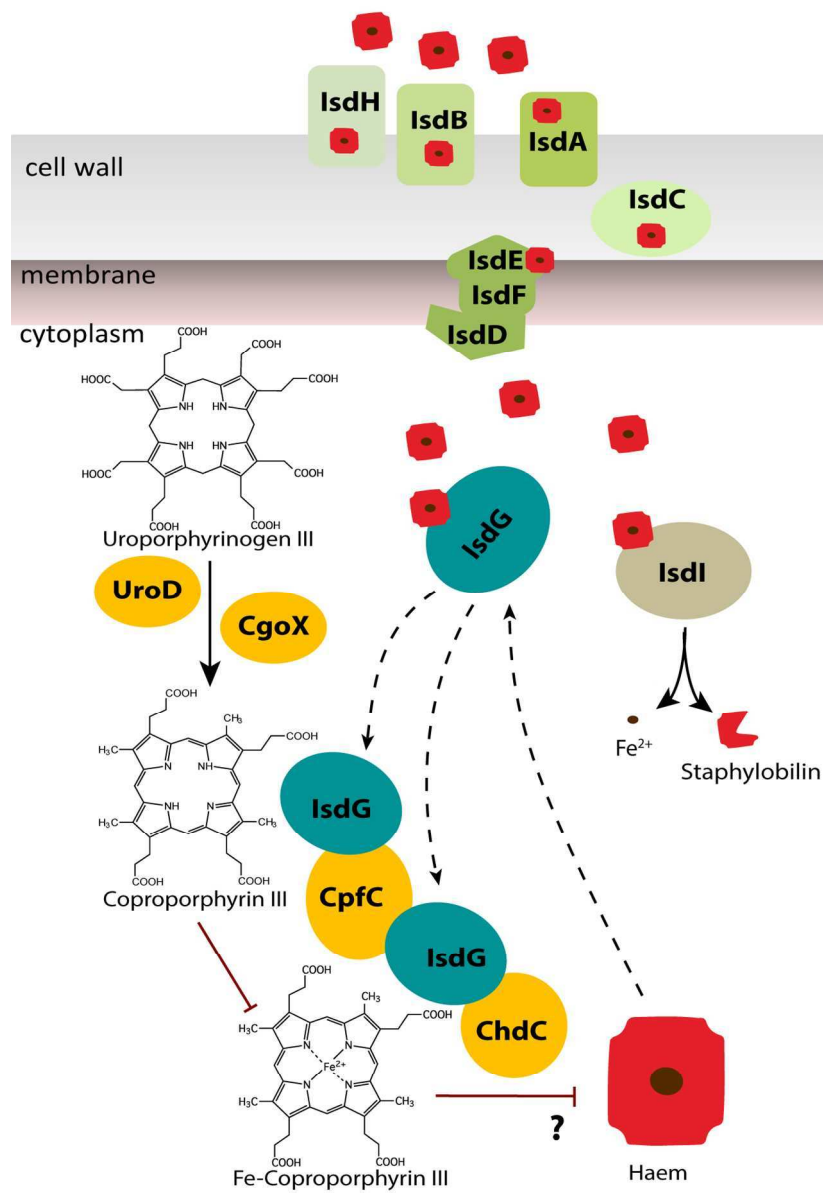
If you believe this document infringes copyright then please contact the KAR admin team with the take-down information provided at <http://kar.kent.ac.uk/contact.html>

Staphylococcus aureus haem biosynthesis and acquisition pathways are linked by haem monooxygenase IsdG

Journal:	<i>Molecular Microbiology</i>
Manuscript ID	MMI-2018-16976.R2
Manuscript Type:	Research Article
Date Submitted by the Author:	n/a
Complete List of Authors:	Videira, Marco; Instituto Tecnologia Química e Biológica, Biologica Chemistry Lobo, Susana; Universidade Nova de Lisboa, Instituto de Tecnologia Química e Biológica António Xavier Silva, Liliana; Instituto Tecnologia Química e Biológica, Biologica Chemistry Palmer, David; University of Kent, Biological Sciences Warren, Martin; University of Kent, Biosciences; Prieto, Manuel; Universidade de Lisboa Instituto Superior Tecnico, Chemistry Coutinho, Ana ; Universidade de Lisboa Instituto Superior Tecnico, Chemistry Sousa, Filipa; University Wien, Biology Fernandes, Fabio; Universidade de Lisboa Instituto Superior Tecnico, Chemistry Saraiva, Ligia; Instituto Tecnologia Química e Biológica, Biologica Chemistry;
Key Words:	haem biosynthesis, ferroxidase, S. aureus, haem uptake, haem monooxygenase

Abbreviated Summary

Haem is an essential cofactor that in pathogens is obtained by means of an internal haem biosynthesis pathway and/or from the host by a capture system. Here it is shown for the first time that pathogens possessing the two systems communicate through a haem monooxygenase enzyme of the LsdG-family type. The importance of this crosstalk lies in the need for pathogens to reconcile their high haem requirements with the paradox that free haem is toxic.



111x163mm (300 x 300 DPI)

1 ***Staphylococcus aureus* haem biosynthesis and acquisition pathways are linked through haem**
2 **monooxygenase IldG**

3

4

5 Marco A.M. Videira¹, Susana A.L. Lobo^{1,2}, Liliana S.O. Silva¹, David J. Palmer³, Martin J. Warren³, Manuel
6 Prieto⁴, Ana Coutinho^{4,5}, Filipa L. Sousa⁶, Fábio Fernandes^{4,7}, and Lúcia M. Saraiva^{1*}

7

8 ¹ Instituto de Tecnologia Química e Biológica António Xavier, Universidade Nova de Lisboa, Avenida da
9 República , 2780-157 Oeiras, Portugal.

10 ² iBET, Instituto de Biologia Experimental e Tecnológica, Oeiras, Portugal. Avenida da República (EAN),
11 2780-157 Oeiras, Portugal (present address).

12 ³ School of Biosciences, University of Kent, Giles Lane, Canterbury, Kent CT2 7NJ, United Kingdom.

13 ⁴ Centro de Química-Física Molecular and Institute of Nanoscience and Nanotechnology, Instituto
14 Superior Técnico, Universidade de Lisboa, Lisboa, Portugal.

15 ⁵ Departamento de Química e Bioquímica, Faculdade de Ciências, Universidade de Lisboa, Lisboa,
16 Portugal.

17 ⁶ Department of Ecogenomics and Systems Biology, University of Vienna, 1090 Vienna, Austria.

18 ⁷ Research Unit on Applied Molecular Biosciences–Rede de Química e Tecnologia (UCIBIO-REQUIMTE),
19 Departamento de Química, Faculdade de Ciências e Tecnologia, Universidade Nova de Lisboa, Caparica,
20 Portugal.

21

22

23

24

25 ****Corresponding author:***

26 Instituto de Tecnologia Química e Biológica António Xavier, UNL

27 Av. da República (EAN)

28 2780-157 Oeiras

29 Portugal

30 Tel: +351 21 4469328

31 Fax: +351 21 4433 644

32 email: lst@itqb.unl.pt

33

Abstract

35

36 Haem is an essential cofactor in central metabolic pathways in the vast majority of living systems.
37 Prokaryotes acquire haem via haem biosynthesis pathways, and some also utilize haem uptake systems,
38 yet it remains unclear how they balance haem requirements with the paradox that free haem is toxic.
39 Here, using the model pathogen *Staphylococcus aureus*, we report that LsdG, one of two haem
40 oxygenase enzymes in the haem uptake system, inhibits the formation of haem via the internal haem
41 biosynthesis route. More specifically, we show that LsdG decreases the activity of ferrochelatase and
42 that the two proteins interact both *in vitro* and *in vivo*. Further, a bioinformatics analysis reveals that a
43 significant number of haem biosynthesis pathway containing organisms possess an LsdG-homologue and
44 that those with both biosynthesis and uptake systems have at least two haem oxygenases. We conclude
45 that LsdG-like proteins control intracellular haem levels by coupling the two pathways. LsdG is thus a
46 novel target for the treatment of *S. aureus* infections.

47

48

49

50

51

52

53

54

55

56

57

58

59

60

61

62

63

64

65

66

67

68

69

70

71 Introduction

72

73 In all forms of life, the ability to perform redox reactions is crucial, often requiring compounds with
74 metal centres and cofactors that are evolutionarily ancient. Haem is an iron-based redox centre that is
75 widely distributed in living organisms and which permits an extensive range of proteins and enzymes to
76 function in essential cellular processes such as aerobic and anaerobic respiration, detoxification,
77 microRNA processing and regulation of gene expression (Choby and Skaar, 2016). Haem is obtained by
78 either *de novo* synthesis (via haem biosynthesis pathways) or by uptake from the environment. Several
79 pathogens extract haem from their host's haemoglobin, which upon degradation serves as a source of
80 iron to satisfy the nutritional needs of the pathogen (Anzaldi and Skaar, 2010; Choby and Skaar, 2016).
81 Furthermore, a large number of microorganisms combine pathways for the endogenous production of
82 haem with complex haem uptake systems.

83 Prokaryotes utilise one of three distinct haem biosynthesis pathways, all of which have common early
84 steps that lead to the intermediate uroporphyrinogen III (Fig. 1). Thereafter, the three distinct routes are
85 referred to as the protoporphyrin, sirohaem and coproporphyrin branches, reflecting intermediates that
86 are unique to each pathway, and the genes involved were recently renamed (Dailey *et al.*, 2017). The
87 protoporphyrin dependent (PPD) branch, previously known as classic pathway, operates in many Gram-
88 negative bacteria. This pathway involves the decarboxylation of uroporphyrinogen III to
89 coproporphyrinogen III by UroD (formerly HemE), followed by decarboxylation to protoporphyrinogen IX
90 by CgdH/CgdC (formerly HemN/HemF) and then oxidation to protoporphyrin IX by PgoX/PgdH1
91 (formerly HemY/HemG) prior to metal insertion by ferrochelatase PpfC (formerly HemH) to give
92 protohaem (Heinemann *et al.*, 2008; Dailey *et al.*, 2017). The sirohaem dependent branch (SHD),
93 originally named the alternative haem biosynthesis pathway Ahb, is active in sulphate-reducing
94 proteobacteria and archaea, transforms uroporphyrinogen III to protohaem via sirohaem in an oxygen-
95 independent process requiring four-enzymatic steps involving the enzymes AhbA-D (Bali *et al.*, 2011;
96 Lobo *et al.*, 2012). The most recently discovered branch, namely the coproporphyrin dependent (CPD)
97 pathway is active in several Gram-positive organisms including *S. aureus* (Lobo *et al.*, 2015). This
98 pathway involves the conversion of uroporphyrinogen III to coproporphyrinogen III by UroD (formerly
99 HemE) and subsequent oxidation to coproporphyrin III by CgoX (formerly HemY). Insertion of iron into
100 coproporphyrin III to make coprohaem is mediated by CpfC (formerly HemH), and the final step involves
101 the decarboxylation of coprohaem to protohaem by ChdC (formerly HemQ) (Dailey *et al.*, 2015; Lobo *et al.*,
102 2015). Although these ferrochelatases catalyse the insertion of iron in a porphyrin ring, the substrate
103 that they act upon is different, being protoporphyrin IX for PPD, coproporphyrin III for CPD and
104 sirohydrochlorin for SHD pathways.

105 The mechanisms of haem biosynthesis in prokaryotes vary widely (Dailey *et al.*, 2017) and control over
106 the pathway has been reported to be regulated by iron, oxygen, reactive oxygen species and by its final
107 product haem (Choby and Skaar, 2016; Dailey *et al.*, 2017). In the case of the latter, the binding of haem
108 to GtrR (formerly HemA), the first enzyme of the pathway, is thought to control the system via a

109 feedback inhibition mechanism (McNicholas *et al.*, 1997; Wang *et al.*, 1997; Choby and Skaar, 2016). The
110 most common haem acquisition system in Gram-positive pathogens is the iron-regulated surface
111 determinant (Isd). *S. aureus* also contains an additional haem transport system (Hts) that, like the Isd
112 proteins, was first described in this bacterium (Mazmanian *et al.*, 2003; Skaar EP, Humayun M, Bae T,
113 DeBord KL, 2004). The Isd system includes the cell wall-anchored proteins IsdA, IsdB, IsdC and IsdH, as
114 well as the haem-binding protein and permease components IsdD, IsdE, and IsdF, and the
115 transmembrane ABC transporter HtsABC (Mazmanian *et al.*, 2003; Skaar EP, Humayun M, Bae T, DeBord
116 KL, 2004). Once haem is transported into the cytoplasm, it is either degraded by the haem
117 monooxygenases IsdG and IsdI to release iron (Skaar *et al.*, 2004), or becomes bound to membrane-
118 associated proteins to act as a cofactor in, for example, electron transport (Thöny-Meyer, 1997). *S.*
119 *aureus* also possesses the haem regulated transporter (HrtAB), an efflux pump that protects cells from
120 haem toxicity (Stauff *et al.*, 2008).

121 *S. aureus* is clinically significant as it is responsible for a large number of human infections including
122 respiratory, urogenital, skin burn-associated and systemic infections (Tarai *et al.*, 2013). It is also a
123 widely studied Gram-positive pathogen and the paradigm for the CPD pathway operating alongside a
124 haem acquisition system. Genes encoding enzymes of the CPD pathway are organized into two operons
125 in *S. aureus*, *gtrR-hemX-hmbS-uroS-pbgS* and *uroD-cpfC-cgoX*, whereas *chdC* is isolated elsewhere in the
126 genome (Lobo *et al.*, 2015). The *S. aureus* haem acquisition system is formed by single units *isdA*, *isdB*,
127 *isdH*, *isdI* and the operon *isdCDEF-srtB-isdG* (Mazmanian *et al.*, 2003; Skaar and Schneewind, 2004). Like
128 many other organisms, *S. aureus* encodes two haem monooxygenases, IsdG and IsdI, which share
129 approximately 70% amino acid identity and which bind and degrade haem to produce iron and
130 staphylobilin (Skaar *et al.*, 2004; Reniere *et al.*, 2010).

131 In this work, we investigated how *S. aureus* controls intracellular haem levels. We show that the haem
132 monooxygenase, IsdG, provides a link between the haem biosynthesis and uptake pathways in *S. aureus*
133 and that this protein prevents excessive formation of toxic haem inside bacterial cells.

134

135

136 Results

137

138 The haem monooxygenase IsdG interferes with haem formed via the haem biosynthesis pathway

139

140 To analyse the role of the two haem monooxygenases of *S. aureus*, the *S. aureus* CPD pathway was
 141 reconstituted in a haemin auxotrophic strain of the Gram-negative bacterium *E. coli* that is deficient in
 142 protoporphyrin ferrochelatase $\Delta ppfC$ (formerly $\Delta visA$ or $\Delta hemH$). As *E. coli* does not take up exogenous
 143 haem through an Isd system, this host represents a good model to study the role of IsdG/I enzymes
 144 without the interference of an endogenous haem acquisition system, thus avoiding the use of *S. aureus*
 145 strains containing multiple mutations. The genes encoding the last three enzymes of the *S. aureus* CPD
 146 pathway, *cgoX-cpfC-chdC*, were cloned by the Link and Lock method (McGoldrick *et al.*, 2005), expressed
 147 in the presence of either IsdG or IsdI in *E. coli* $\Delta ppfC$, and growth of the complemented strain was
 148 monitored. The results showed that expression of CgoX-CpfC-ChdC alone abolished the haem auxotrophy
 149 of the strain, which grows similar to an *E. coli* wild type strain. However, in the presence of either IsdG or
 150 IsdI, the growth of the strain was impaired (Fig. 2A).

151 In order to understand the growth behaviour of the complemented strains, the tetrapyrrole products
 152 formed during the expression of *S. aureus* *cgoX-cpfC-chdC* genes in the presence of IsdI or IsdG were
 153 analysed by HPLC-MS. As expected, cells expressing *S. aureus* CgoX-CpfC-ChdC exhibited a peak with a
 154 mass-to-charge ratio (m/z) of 616, confirming their ability to produce haem. However, this peak
 155 significantly decreased when IsdG or IsdI were also expressed (Fig. 2B), with cells expressing *S. aureus*
 156 CgoX-CpfC-ChdC-IsdI containing approximately 3 times less haem, and cells expressing CgoX-CpfC-ChdC
 157 together with IsdG showing no detectable peak corresponding to haem. These results suggest that the
 158 haem monooxygenases interfere with the haem formation *in vivo*.

159 The lack of growth in the presence of IsdG/I enzymes indicated that no haem was being formed, which
 160 could result from degradation and/or inhibition of its formation. To test these possibilities, we analysed
 161 the growth of *E. coli* $\Delta ppfC$, complemented with its own ferrochelatase PpfC and in the presence of IsdI
 162 or IsdG. Under these conditions where the haem is formed through the PPD pathway, it was observed
 163 that only IsdI impaired the growth while IsdG had no effect (Fig. 2C).

164 Hence, we conclude that IsdI always acts as a haem monooxygenase as it degrades haem independently
 165 of whether it is formed by the CPD or PPD pathways while IsdG impairs the growth of the strain using
 166 the CPD pathway but not of the strain using the PPD pathway suggesting that IsdG is not acting as a
 167 haem degrading enzyme.

168

169

170 IsdG decreases the ferrochelatase activity of CpfC

171

172 To understand how the *S. aureus* IsdG and IsdI constrain the CPD pathway, we tested whether they
 173 interfere with the activity of the *S. aureus* ChdC enzyme that catalyses the last step of the CPD branch
 174 promoting the conversion of iron-coproporphyrin III into haem in the presence of its electron acceptor

(Lobo *et al.*, 2015). Thus, *S. aureus* ChdC was incubated with iron-coproporphyrin III in the presence of either IsdG or IsdI and hydrogen peroxide. However, control experiments performed in the absence of ChdC showed that hydrogen peroxide activates the inherent peroxidase activity in IsdG and IsdI, leading to degradation of the iron-coproporphyrin III substrate (Fig. S1). We therefore shifted our attention to the penultimate enzyme of the CPD branch, the ferrochelatase CpfC, which plays an important role in the survival of *S. aureus* (Fig. S2), as also shown for the GtrR and PbgS enzymes involved in the first steps of the CPD pathway (Hammer *et al.*, 2013; Hammer *et al.*, 2014).

In *S. aureus* and other Gram-positive operating via the CPD pathway, the ferrochelatase incorporates iron into coproporphyrin III to form iron-coproporphyrin III, which is then sequentially decarboxylated by ChdC to yield protohaem. We observed that the cell lysate of *S. aureus* *cpfC* mutant contained very low levels of cellular catalase activity, which was restored to wild type level upon addition of external haemin (Fig. S3). It was previously reported that the total cellular catalase activity was lower in *S. aureus* *pbgS* and *chdC* defective strains (Mayfield *et al.*, 2013). We next tested whether the haem monooxygenases impaired ferrochelatase activity. *S. aureus* CpfC, IsdG and IsdI were recombinantly produced and purified, yielding stable proteins that had the expected molecular masses of approximately 35 and 12.5 KDa, respectively (data not shown). *S. aureus* ferrochelatase activity was determined by following the depletion of coproporphyrin III, which yielded a specific activity of 234 ± 14 nmol.min⁻¹mg⁻¹. While addition of IsdI to the reaction mixture caused no significant alteration (Fig. 3A), the presence of IsdG led to a ~50% decrease in ferrochelatase activity. Furthermore, the activity of the enzyme decreased with increasing concentration of IsdG (Fig 3B).

These results show that IsdG, but not IsdI, attenuates the activity of the *S. aureus* CpfC. Therefore, we next determined the haem cellular content in cells forming haem by the CPD pathway in the presence and absence of IsdG. For this purpose, *S. aureus* wild type and Δ *isdG* mutant cells were grown in the presence of aminolaevulinic acid, the first stable precursor of the haem biosynthesis pathway. Figure 3C shows that the IsdG inactivated strain has significantly higher haem content. Therefore, we conclude that IsdG impairs CpfC lowering the amount of haem formed by the CPD pathway.

Protein-protein interaction studies between IsdG and CpfC

We reasoned that the inhibition of the *S. aureus* CpfC activity by IsdG is most likely a result from a direct interaction between the two proteins. Three type of experiments were done; pull down assays, Förster resonance energy transfer (FLIM-FRET) and fluorescence polarization binding experiments.

For the pull down assays, purified CpfC-His tagged protein bound to a Ni-Sepharose column was incubated with cells extracts expressing IsdG or IsdI. The bound proteins were eluted with imidazole containing buffer and separated electrophoretically. As visualised by SDS-PAGE, IsdG is pulled down

212 together with CpfC, while IsdI does not bind to the column-loaded CpfC (Fig. 4A). Hence, the results
213 show that there is a specific interaction between CpfC and IsdG.

214

215 To further study this interaction *in vivo* fluorescence lifetime imaging based Förster resonance energy
216 transfer (FLIM-FRET) was used. Additionally, interactions among the various CPD pathway protein
217 components and *S. aureus* haem monooxygenases were also evaluated. In order to do this, we
218 constructed *S. aureus* CpfC and ChdC proteins fused to a GFP donor molecule and IsdG, IsdI, ChdC and
219 CpfC fused to a mCherry acceptor molecule (Table S1).

220 The interaction between IsdG and CpfC was analysed in bacterial cells expressing *S. aureus* CpfC-GFP and
221 IsdG-mCherry. CpfC-GFP exhibited a mono-exponential fluorescence decay with a lifetime $\tau_{\text{CpfC-EGFP}} = 2.2$
222 ± 0.1 ns (Fig S4). In the presence of IsdG-mCherry, the fluorescence decay of CpfC-GFP was no longer
223 accurately described by a single exponential and a shorter component had to be included in the fit,
224 indicating the presence of FRET and thus an interaction between the two proteins (Fig. 4 and Fig S4). The
225 FRET efficiencies (*E*) were dependent on the concentration of IsdG, according to the plots of *E* against
226 mCherry/GFP fluorescence intensity ratios (Fig. 4), obtained from the confocal fluorescence
227 measurements of each construct (see Methods).

228 Although some degree of interaction between CpfC-GFP and IsdI-mCherry was also detected (Fig. 4B
229 and 4D), the FRET efficiencies determined for this protein pair were much lower than those measured
230 for IsdG and CpfC (Fig. 4C), suggesting a much less efficient interaction. Furthermore, an interaction
231 between ChdC and IsdG, but not ChdC and IsdI, was also observed (Fig. 4E and 4F).

232 Together, these data reveal that IsdG interacts with the last two enzymes of the CPD pathway, namely
233 CpfC and ChdC.

234

235 The FLIM-FRET protein-protein interaction studies were complemented with an *in vitro* homogeneous
236 fluorescence polarization binding assay to monitor macromolecular complex formation between the
237 two recombinant *S. aureus* proteins, CpfC and IsdG. For this purpose, *S. aureus* CpfC was covalently
238 conjugated to dansyl chloride, a long-lived fluorescent probe, in order to evaluate its binding to IsdG
239 using both steady-state and time-resolved fluorescence anisotropy measurements (Valeur and
240 Berberan-Santos, 2012). The dansyl-labeled CpfC gave a high steady-state fluorescence anisotropy in
241 solution ($\langle r \rangle = 0.164 \pm 0.002$; Fig. 4G and Fig. S5). Upon increasing the concentration of dimeric IsdG in
242 solution, the steady-state fluorescence anisotropy of dansyl-CpfC steadily augmented (Fig. S6) reaching a
243 plateau level of $\langle r \rangle \sim 0.20$ (Fig. 4G). In contrast, there was negligible binding observed between IsdI
244 and CpfC. Upon binding of dimeric IsdG to dansyl-labeled CpfC, the hydrodynamic volume of the protein
245 complex increased, slowing down the overall rotational tumbling of dansyl-labeled CpfC in solution
246 during its excited-state fluorescence lifetime and ultimately producing an increase in its steady-state
247 fluorescence anisotropy (Jameson and Ross, 2010; Valeur and Berberan-Santos, 2012). These data were
248 further corroborated by time-resolved polarized fluorescence measurements of dansyl-labeled CpfC
249 during its titration with IsdG. The fluorescence anisotropy decay of dansyl-labeled CpfC was greatly

affected by addition of IsdG to the solution (Fig. S6). In particular, the longer rotational correlation time, ϕ_2 , assigned to the overall rotational motion of dansyl-labeled CpfC in solution, increased significantly from $\phi_2 \sim 67$ ns for dansyl-labeled CpfC free in solution to $\phi_2 \sim 180$ ns for dansyl-labeled CpfC in the presence of 107 μ M IsdG (Fig. 4H and Table S2). A binding K_d of 14.3 ± 2.6 μ M (for the dimeric form of IsdG) and a $\langle r \rangle_B$ of 0.207 ± 0.003 was determined. These results clearly demonstrate that IsdG has the ability to bind to CpfC in solution at physiological pH.

Haemin increases IsdG expression

To assess the impact of haem uptake by the host to its endogenous haem biosynthesis, we determined the expression of the haem biosynthesis genes in *S. aureus* cells grown in medium supplemented with haemin (2.5 μ M). Addition of external haemin modified the mRNA content of *gtrR*, *uroD* and *chdC* (Fig. 5A). A similar change was observed with the genes encoding the iron-regulated surface determinants *isdA*, *isdB* and *isdI*, while *hrtB* and *htsA* were strongly upregulated (Fig. 5A). Treatment with exogenous haemin also caused a significant induction of the *isdCDEG* operon (Fig. 5A).

The pronounced change in *isdG* gene expression led us to analyse the amount of IsdG protein in cells containing excess haem, which was either added exogenously to the medium or produced endogenously through supplementation with aminolaevulinic acid. For this purpose, an IsdG-GFP fusion protein was constructed and the amount of IsdG was determined by the direct measurement of the fluorescence derived from the construct by flow cytometry. For comparative purposes, an IsdI-GFP fusion protein was also constructed. *S. aureus* expressing GFP, IsdG-GFP or IsdI-GFP were grown in either TSB supplemented with haemin or TSB containing an excess of aminolaevulinic acid. Addition of haemin increased the levels of IsdG, which was evidenced by the higher fluorescence of *S. aureus* cells expressing IsdG-GFP compared to cells expressing GFP alone (Fig. 5B). Cells expressing IsdI-GFP showed slightly higher fluorescence than cells expressing GFP alone, however at a much lower extent than cells containing IsdG-GFP (Fig. 5B). Interestingly, addition of aminolaevulinic acid caused an increase in fluorescence, revealing that internally produced haem also augments the cellular content of IsdG (Fig. 5C). In contrast, supplementation with aminolaevulinic acid produced a strong decrease of fluorescence in cells expressing IsdI-GFP. Therefore, the increase in the intracellular content of IsdG promoted by haem may trigger the interaction of IsdG with CpfC with a consequential impairment of the CPD pathway.

IsdG-like proteins are found in organisms that encode haem biosynthesis and lack haem uptake systems

IsdG-type haem degrading monooxygenases are a family of proteins that are characterized by the presence of an antibiotic biosynthesis monooxygenase (ABM) domain followed by a loop region

(Reniere *et al.*, 2011). To further test our proposal that IsdG-like proteins play a role in haem biosynthesis, we analysed the distribution of these proteins in complete and annotated genomes and their co-occurrence with genes encoding haem biosynthesis and/or haem uptake systems. For this purpose, an organism was considered to have a *de novo* haem biosynthesis ability if at least 75% of the pathway was encoded in its genome. For the PPD pathway, besides the 75% rule either CgdC or CgdH had to be present in the organism's genome. In addition, for organisms with the CPD pathway, ChdC had to be encoded in the genome. Also, an organism was considered to be able to perform haem uptake if its genome encoded a complete transport system with at least one haem binding protein (HmuT, IsdE or RV2003) (see Methods).

Data showed that among the so far complete and annotated genomes (5060) more than 1/5 of the organisms contain genes encoding IsdG-like proteins (Supplementary Data 1). The IsdG-like proteins are more represented in Gram-positive organisms (79%) (Fig. 6A). The majority of IsdG-like containing organisms encode complete (or almost complete) haem biosynthesis and uptake systems (Fig. 6B). Interestingly, IsdG-like proteins were not found in organisms that synthesize haem through the alternative haem biosynthesis pathway.

Within the 747 Gram-positive organisms that perform both haem biosynthesis and uptake, 422 (~56%) contained two or more genes coding for IsdG-like proteins. The remaining genomes contain only one IsdG-type protein but in ~50% of these organisms IsdG occurs together with genes coding for other haem monooxygenases belonging to the HemO, HmuO, ChuS/HmuS or HugZ families of haem monooxygenases (Fig. 6C). Within the 108 Gram-negative organisms, the majority (81%) encode two haem monooxygenases.

Noteworthy, IsdG-like proteins are found in organisms that lack haem uptake systems but contain haem biosynthesis pathways. Moreover, over 90% of the organisms that apparently have incomplete haem biosynthesis or uptake systems encode IsdG homologues together with haem biosynthesis ChdC and/or CpfC associated enzymes. These organisms belong to *Lactobacillus plantarum* or *Lactobacillus reitti* species that are unable to perform haem biosynthesis, but when grown with haem (and menaquinone), couple their haem-independent fermentative metabolism with aerobic respiration (Brooijmans *et al.*, 2009).

Altogether, the analysis showed that among the IsdG containing bacteria many of these organisms seem to rely only on haem biosynthesis pathways. Moreover, even the genomes that lack genes putatively involved in haem biosynthesis or uptake pathways still encode IsdG, ChdC and CpfC-like genes. Finally, the majority of the organisms with well-defined haem biosynthesis and uptake pathways contain two haem monooxygenases-like proteins, which supports the hypothesis that one haem monooxygenase could be used for haem degradation and the other could potentially interfere with haem biosynthesis, as shown in this work for *S. aureus*.

Discussion

We have investigated the way in which prokaryotes that obtain haem through haem biosynthesis and uptake pathways balance their high haem needs with the toxicity associated with free haem. We have shown that IsdG, one of the haem monooxygenases in the *S. aureus* haem uptake pathway, controls intracellular haem content through a protein-protein interaction with ferrochelatase that results in inhibition of iron-coproporphyrin chelatase activity. A comprehensive bioinformatics analysis showed that IsdG-like proteins are present in a significant number of prokaryotes that contain only the haem biosynthesis pathway. Altogether, the data allows us to propose that the IsdG protein family is not only the missing link between the two pathways, but also acts as the brake that avoids production of undesirably high intracellular haem levels.

In several microorganisms, IsdG-type haem monooxygenases, including the *S. aureus* IsdG and IsdI, have been assigned a haem-degradation role *in vitro* (Skaar *et al.*, 2004), and are required for growth when haemin is the only available iron source (Reniere and Skaar, 2008). We observed that IsdI impairs growth when haem is formed through PPD or CPD pathways, which is consistent with the haem degrading activity of IsdI. In contrast, IsdG inhibited growth only when haem was generated by the CPD pathway, which suggests that IsdG interferes with the haem synthesis pathway.

Experimentally, we have demonstrated that strains containing IsdG have lower amounts of intracellular haem formed via the haem biosynthesis route and IsdG has the ability to decrease the iron-coproporphyrin chelatase activity of *S. aureus* CpfC. Furthermore, we showed by *in vivo* FLIM-FRET and fluorescence polarization binding assays that the two proteins interact and have generated a model for this interaction.

Under our conditions, addition of haem did not repress expression of the *S. aureus* CPD pathway linked genes, as has been reported previously for several organisms. The only exception to this observation is with the *Corynebacterium diphtheriae gtrR*, which is repressed under haem replete conditions (Bibb *et al.*, 2007). Thus, in general, haem does not serve as a feedback factor to repress its own synthesis at the transcriptional level. Haem toxicity in *S. aureus* has previously been associated with induction of the

364 haem regulator transporter HrtAB (Torres *et al.*, 2007). In agreement with this, when we treated
365 cells with haemin, they exhibited induction of the first gene of the *hrtBA* operon. More
366 significantly, we observed that expression of *isdG* was highly upregulated, indicating that IsdG may
367 play a role in haem regulation. Furthermore, this upregulation translated into an increase of the IsdG
368 protein abundance, as shown by FACS. Consistent with our results, IsdG, but not IsdI, has been reported
369 to be regulated at the post-transcriptional level such that it is stabilized in the presence of haem and
370 undergoes proteolytic degradation in the absence of haem (Reniere and Skaar, 2008; Reniere *et al.*,
371 2011). We observed a higher abundance of IsdG in *S. aureus* when it was grown in iron-replete
372 medium, while other authors have reported that IsdG is more expressed upon addition of exogenous
373 haemin to iron-starved cultures of *S. aureus* (Reniere and Skaar, 2008). These differences are most
374 probably due to the experimental conditions used in the two assays.

375

376 The bioinformatics analysis reported in this work estimates that among bacteria that only synthesize
377 haem endogenously approximately one third contain IsdG-like proteins. Even in organisms with a less
378 well-defined haem biosynthesis pathway, IsdG-type enzymes coexist with ChdC and/or CpfC enzymes
379 (Fig. S6B). This is in agreement with previous studies that have shown that the presence of IsdG is not
380 restricted to organisms that have both the haem biosynthesis and acquisition machineries (Sousa *et al.*,
381 2013). However, in many cases the genes encoding for IsdG-like enzymes are co-localised with genes for
382 PPD and CPD pathways. Hence, IsdG may regulate both these routes for endogenous biosynthesis
383 of haem. Our data support the proposal that in *S. aureus* this control occurs through the interaction of
384 IsdG with CpfC, as the presence of IsdG strongly decreases ferroxidase activity and the intracellular
385 haem abundance. Although at this stage the interaction at the molecular level between IsdG and CpfC
386 cannot be fully described due to the lack of detailed structural information, we hypothesize that this
387 interaction may block the access of the substrate to the porphyrin binding cleft of CpfC.

388

389 Until now there has been a great deal of focus on the mechanisms of haem uptake as a source of iron,
390 whilst the question of how microbes prevent unwanted haem toxicity by fine tuning
391 exogenously acquired haem with haem synthesized endogenously remains less understood.

392

393

394 The scheme depicted in Fig. 7 summarises our current proposal for bacteria to maintain their
395 intracellular free haem pool below hazardous levels. Organisms with both haem biosynthesis and uptake
396 systems use external haem in two different ways. External haem is transported into the cytoplasm
397 through dedicated systems, including those of the Isd-type, where it is either directly incorporated into
398 apo-haemoproteins or degraded by IsdI, HemO, HmuO, ChuS/HmuS or HugZ- like proteins to release
399 iron. On the other hand, haem also increases the abundance of IsdG to levels that are sufficient to
400 interact with CpfC blocking its function, i.e, impairing the haem biosynthesis pathway. Hence, one of the
401 haem monooxygenase enzymes would likely be dedicated to haem degradation to provide a source for

iron whilst the other would act to restrain internal haem biosynthesis. Moreover, in systems that only synthesize haem via an internal haem biosynthesis pathway and contain IsdG-like proteins, IsdG may play an important role in preventing excessive production of haem.

Collectively, our results show that the haem uptake and biosynthesis are not independent processes, and that IsdG-like proteins have a role in the crosstalk between these two systems which allow bacteria to adapt to a range of environments while avoiding haem toxicity. Therefore, we predict that the design of inhibitory drugs targeting the IsdG family of proteins will have a significant therapeutic benefit for the treatment of pathogenic infections.

Experimental Procedures

Strains and growth conditions

The strains used in this work are listed in Supplementary Table 3 and were grown under aerobic conditions, at 37 °C and 150 rpm. *S. aureus* was cultured in tryptic soy broth (TSB), with the exception of the cells that were used for RNA extraction that were cultured in Roswell Park Memorial Institute (RPMI) medium supplemented with 1% casamino acids. *E. coli* strains were grown in Luria-Bertani (LB), except *E. coli* expressing the pWhiteWalker plasmid that was grown in Brain Heart Infusion (BHI) medium. Selection was achieved by addition of the indicated antibiotics, namely kanamycin (50 µg ml⁻¹), erythromycin (20 µg ml⁻¹ or 400 µg ml⁻¹ for FRET experiments) and ampicillin (100 µg ml⁻¹).

RNA isolation and quantitative real-time RT-PCR assays

Overnight cultures of *S. aureus* were diluted to an optical density at 600 nm (OD₆₀₀) of 0.1 on RPMI containing 1% casamino acids or RPMI containing 1% casamino acids supplemented with haem (2 µM). Cells at an OD₆₀₀ = 1 were treated with an ice-cold ethanol/phenol RNA protective solution (5%), centrifuged at 2000 x g for 5 min, and the pellets flash frozen in liquid nitrogen. For RNA isolation, pellets were thawed on ice, resuspended in 10 mM Tris pH 8 and lysed with 2 mg ml⁻¹ lysozyme and 30 µg ml⁻¹ lysostaphin at 37 °C, for 30 min. The lysates were transferred to Aurum RNA Binding Mini Columns and total RNA was extracted using Aurum™ Total RNA Mini Kit (Bio-Rad), following the manufacturer's instructions. Contaminating DNA was removed using Ambion® TURBO DNA-free™ DNase kit (Life Technologies), and RNA concentration and purity were evaluated in a Nanodrop ND-1000 UV-visible spectrophotometer (Thermo Fisher Scientific).

435 For the cDNA synthesis, 800 ng of RNA was reverse transcribed with the Transcriptor High Fidelity cDNA
 436 Synthesis Kit (Roche) using the Anchored-oligo (dT)18 and Random Hexamer primers. Quantitative real-
 437 time RT-PCR assays were done in a LightCycler® 480 (Roche) using the oligonucleotides listed in
 438 Supplementary Table 4 and the LightCycler® 480 SYBR Green I Master kit (Roche). Relative quantification
 439 of each gene is shown in relation to the 16S rRNA reference gene, whose expression does not vary
 440 under the tested conditions, and using the comparative C_T method. Assays were done for two
 441 independent biological samples analysed in triplicate.

442 **Gene cloning**

443 The genes encoding *S. aureus* Newman IsdG and IsdI were amplified, by standard PCR reactions, from
 444 genomic DNA using the Phusion High-Fidelity DNA Polymerase (Thermo Fischer) and the
 445 oligonucleotides described in Supplementary Table 4. DNA fragments were cloned into either pET-23b
 446 or pET-28a vectors (Novagen) to produce wild type proteins and N-terminal His-Tag fused proteins,
 447 respectively. All plasmids were confirmed for gene integrity by DNA sequencing.

448 For the complementation experiments, plasmid pET-23b containing combinations of *cpfC*, *chdC*, *cgxX*,
 449 *isdG*, *isdI* of *S. aureus* (*Sa*), namely pET-23b-*SacgoXcpfCchdCisdG*, pET-23b-*SacgoXcpfCchdCisdI*, were
 450 generated by the link and lock methodology (McGoldrick *et al.*, 2005).

451 For the Förster Resonance Energy Transfer (FRET) studies, the *isdG*, *isdI*, *cpfC* and *chdC* genes amplified
 452 from *S. aureus* genomic DNA, as described above, were cloned into pBCB plasmids, which were kindly
 453 provided by Mariana Pinho (ITQB-NOVA, Portugal).

454 CpfC and ChdC proteins fused at the N-terminal to GFP were generated by cloning the respective genes
 455 into SphI/SpeI-pBCB1-*gfp* vector whereas IsdG, IsdI, CpfC and ChdC were fused at the C-terminal to
 456 mCherry (mCh) by cloning into the KpnI/NheI-pBCB7-*mCh* vector. After confirmation of the correct
 457 sequence of the fusion genes, BL21(DE3)Gold cells were used as recipient for the generated plasmids
 458 and analysed by FRET.

459 For the flow cytometry experiments, the *S. aureus isdG* gene was cloned into the EcoRI/KpnI restriction
 460 sites of pWhiteWalker3 (kind gift of Simon Foster, University of Sheffield, UK) to generate the in-frame
 461 fusion *isdG-gfp* (pWW-*isdG-gfp*). Plasmid pWhiteWalker3 that expresses only GFP (pWW-*gfp*) was also
 462 constructed to be used as control. For this purpose, a gBlock gene fragment of 244 bp that includes a
 463 ribosomal binding site and the N-terminal sequence of GFP (Integrated DNA Technologies) was cloned
 464 into EcoRI/NcoI-pWW-*isdG-gfp*. The correct sequence of the two recombinant plasmids was confirmed,
 465 and after electroporation into *S. aureus* the fluorescence level of GFP was analysed by flow cytometry.

466 Complementation experiments

467 Plasmid pET-23b harbouring combinations of genes of *S. aureus* *cgoX*, *cpfC*, *chdC*, *isdG*, *isdI*, and *E. coli*
468 *ppfC* were transformed into competent cells of *E. coli* ferrochelatase mutant $\Delta ppfC$ (formerly $\Delta visA$, kind
469 gift from Mark O'Brian, State University of New York at Buffalo, New York, USA) (Frustaci and O'Brian,
470 1993). Overnight cultures were grown in LB supplemented with ampicillin and 5 μ M haemin and 1 ml
471 aliquots of cells were centrifuged at 1700 $\times g$ for 5 min and washed three times with LB. These pellets
472 were used to inoculate LB-ampicillin, and growth was monitored for 8 h by measuring the optical density
473 at 600 nm (OD_{600}) in a spectrophotometer (Multiskan™ GO, ThermoFisher Scientific). Assays were done
474 for two independent biological samples.

475 Infection assays

476 Murine macrophages J774A.1 (5×10^5 cells/ml) (LGC Promochem) were cultured in Dulbecco's modified
477 Eagle's medium (DMEM) supplemented with 10% of fetal bovine serum, 100 μ M of non-essential amino
478 acids (Gibco), 50 U ml⁻¹ of penicillin (Gibco), and 50 μ g ml⁻¹ of streptomycin (Gibco) in 24-well plates, at
479 37°C in a 5% CO₂-air atmosphere. Prior to infection, macrophages were activated with 5 μ g ml⁻¹ LPS
480 (Sigma) and 1 μ g ml⁻¹ IFN- γ (Sigma), for 5 h. *S. aureus* wild type and $\Delta cpfC$ mutant were inoculated,
481 separately, in TSB medium and grown overnight. The cultures were re-inoculated in TSB, and 4 ml of
482 cells grown to an OD_{600} = 0.4 were centrifuged at 4300 $\times g$ for 5 min, and washed three times with PBS.
483 Cells were then resuspended in DMEM, diluted to $OD=0.05$ ($\sim 10^7$ CFU ml⁻¹) and used to infect the
484 murine macrophages. After 30 min of infection, at 37 °C, cells were washed twice with PBS and
485 incubated with 50 μ g ml⁻¹ of gentamycin, at 37 °C, for 10 min, to prevent extracellular bacterial growth.
486 Immediately after the addition of DMEM (time zero) and 2 and 4 h later, macrophages were collected,
487 lysed with 2% of saponin and the number of intracellular bacteria was determined by CFU counting on
488 TSB agar plates, which also contained 4 μ M haemin to allow for the growth of the ferrochelatase mutant
489 strain. Experiments were done for three independent biological samples assayed in duplicate.

490 Production of recombinant proteins

491 For the purification of *S. aureus* ferrochelatase CpfC, pET-23b-*SahemH* was transformed into
492 BL21STAR(DE3) pLysS (Novagen) competent cells that were grown in LB medium at 37 °C and 150 rpm.
493 Cells at an OD_{600} of 0.6 were induced by addition of 400 μ M of isopropyl β -D-1-thiogalactopyranoside
494 (IPTG) in the presence of 8 mg ml⁻¹ of FeSO₄ and grown for an additional 16-20 h, at 20 °C. For the
495 production of *S. aureus* IsdG and IsdI, plasmids pET-28b-*SaisdG* and pET-28b-*SaisdI* were transformed,
496 separately, in competent cells of *E. coli* BL21(DE3)Gold. Cells were grown in LB medium until reaching an
497 OD_{600} =0.7, and the protein expression was induced by addition of 1 mM of IPTG to the medium, and
498 cells grown at 30°C for 3 h. Cells were harvested by centrifugation (10000 $\times g$, 15 min, 4 °C), and the

pellets were resuspended in 50 mM Tris-HCl pH 7.5 (Buffer A). Cells were disrupted in a French press operating at 1000 Psi, and centrifuged at $27216 \times g$, at 4°C, for 15 min. The supernatant was applied onto a Ni-Sepharose chelating fast flow column (GE Healthcare), previously equilibrated with buffer A supplemented with 10 mM of imidazole, and the proteins were eluted at 400 mM of imidazole and dialysed against buffer A supplemented with NaCl (150-400 mM). Proteins with level of purity >95%, as judged by SDS-PAGE, were concentrated in an Amicon Stirred Ultrafiltration Cell using a 10 kDa membrane (Millipore) and frozen until use.

506

507 **Enzymatic activities**

508 *Catalase activity*

Overnight cultures of *S. aureus* wild type, and $\Delta cpfC$ mutants were grown in TSB only or supplemented with 4 μ M haemin to an OD₆₀₀ of 1. Cells were pelleted by centrifugation ($10000 \times g$, 10 min), resuspended in buffer A and incubated with 7 μ g of lysostaphin for 45 min, at 37 °C. The protein concentration of the cell lysates was determined using the Pierce Bicinchoninic acid Protein Assay (Thermo Scientific) and Sigma protein standards. For the catalase activity assays, approximately 26 μ g of cells lysate proteins were added to buffer A containing 10 mM H₂O₂. The catalase activity was measured by following the decrease in absorbance at 240 nm for the consumption of H₂O₂ ($\epsilon_{240nm} = 43.6 \text{ M}^{-1} \text{ cm}^{-1}$) in a Shimadzu UV-1700 spectrophotometer. Assays were done in triplicate.

517 *Ferrochelatase activity*

The assays were performed under anaerobic conditions in a Coy model A-2463 and Belle Technology chamber equipped with a Shimadzu UV-1800 spectrophotometer. For the preparation of coproporphyrin III (copro III) solution, 1–2 drops of 25% NH₄OH was added to 1-3 mg of copro III powder followed by addition of 1 ml of water. Copro III concentration was determined spectrophotometrically in 0.1 M HCl ($\epsilon_{548} = 16.8 \text{ mM}^{-1} \text{ cm}^{-1}$). For the ferrochelatase assay, CpfC (0.3 μ M) was pre-incubated with IsdI or IsdG (1:10 molar ratio) at room temperature, for 10 min. Next, these proteins were added to the reaction mixture that contained copro III (10 μ M) and (NH₄)₂Fe(SO₄)₂ (10 μ M) in buffer Tris-HCl pH 8.0. The IsdG titration experiments, were performed using IsdG concentrations of 0.3, 0.7, 1.7 and 3.4 μ M, which correspond to 1:1, 1:2, 1:5 and 1:10 stoichiometry relative to the concentration of CpfC. The chelatase activity was measured by following the decrease in absorbance of copro III, measured at 392 nm ($\epsilon_{392nm} = 0.115 \text{ } \mu\text{M}^{-1} \text{ cm}^{-1}$). Assays were done in triplicate.

529

530 Haem abundance assays

531 *S. aureus* wild type and Δ *isdG* mutant cells were grown for 8h and then diluted in TSB in the presence of
532 400 μ M of aminolaevulinic acid. Cells were harvested by centrifugation (8000 x g, 5 min, 4 °C), washed
533 and resuspended in buffer A, and incubated with lysostaphin, at 37 °C, for 45 min. The supernatant was
534 collected by centrifugation and the intracellular haem was quantified essentially as previously described
535 (Wolf *et al.*, 1984; Levicán *et al.*, 2007). Cell extracts (250 μ L) were mixed with the same volume of a
536 solution containing 0.5 M NaOH and 2.5 % Triton-X-100, and the haematin formation was determined
537 measuring the absorbance at 575 nm in a spectrophotometer Shimadzu UV-1700. Haemin from Frontier
538 Scientific was used as standard.
539

540 Mass spectrometry of tetrapyrrole products

541 The plasmids pET-23b containing combinations of *cgoX*, *cpfC*, *chdC*, *isdG* and *isdI* were inserted into *E.*
542 *coli* ferrochelatase mutant Δ *ppfC*. Cells were prepared as described above for the complementation
543 experiments, and inoculated in LB medium to an OD_{600} ~0.05 and grown for 7 h. Cells were harvested by
544 centrifugation at 10000 x g for 10 min, resuspended in buffer A, disrupted at 900 Psi in a French press,
545 and centrifuged at 17000 x g for 30 min, at 4 °C. Protein content of the cell-free lysates was quantified
546 using a Nanodrop ND-2000C (Thermo Scientific). Lysates with the equal protein concentration were
547 treated for haem extraction. Briefly, proteins were precipitated by incubation of lysates with an
548 acetone:HCl (19:1 vol/vol) mixture for 20 min, at room temperature, and removed by centrifugation at
549 14000 x g for 2 min. Following addition to supernatants of 1 ml of cold water, few milligrams of $(NH_4)_2SO_4$
550 (Panreac) and 300 μ l of pure ethyl acetate (Sigma), haem was extracted from the organic phase after
551 centrifugation at 14000 x g for 2 min. Samples were resolved by HPLC-MS on an Ace 5 AQ column
552 attached to an Agilent 1100 series HPLC, equipped with a diode array detector and coupled to a
553 micrOTOF-Q II (Bruker) mass spectrometer. Separation of the products was achieved by applying a
554 gradient composed by 0.1% TFA and acetonitrile, at a flow rate of 0.2 ml min⁻¹. The column was first
555 equilibrated with 20% solvent B, and after sample injection the concentration of solvent B was increased
556 up to 100% during 50 min. Haem quantification was done by measuring the area of absorbance peak at
557 400 nm for m/z 616 (haem).

558 Flow cytometry

559 Overnight cultures of *S. aureus* RN4220 transformed with pWW-*isdG-gfp*, pWW-*isdI-gfp* or pWW-*gfp*
560 were grown in TSB to an OD_{600} ~1.5, diluted to an OD_{600} of 0.1 in TSB supplemented with 10 μ M of IPTG,
561 and grown for one extra hour. At this stage, cells were divided in 10 ml aliquots and grown for 4 h in the
562 absence and in the presence of 5 μ M haemin or 400 μ M of aminolaevulinic acid. Cells (1 ml) were

collected by centrifugation at $11400 \times g$ for 1 min, and the pellets were washed 3 times with PBS, diluted in PBS to an OD_{600} of 0.1 and analysed in a Cell Sorter S3e™ (Biorad). For each sample, at least, 300,000 cells were collected and analysed with the FlowJo programme (Tree Star), and three biological samples were measured for each condition.

567

568 **Fluorescent labelling of CpfC**

S. aureus CpfC was covalently labelled with 5-dimethylaminonaphthalene-1-sulfonyl chloride (dansyl chloride) according to the manufacturer's instructions (Invitrogen). Briefly, recombinantly produced and purified *S. aureus* CpfC (7.5 mg ml^{-1}), solubilized in 0.1 M sodium bicarbonate pH 8.6, was incubated in a 1:1 ratio with dansyl chloride (10 mg ml^{-1} in dimethylformamide) for 1 h at 4°C , in the dark and under continuous stirring. The reaction was quenched by the addition of hydroxylamine (1.5 M, pH 8.5), and the mixture was then loaded onto a PD-10 column (GE Healthcare) equilibrated with buffer A in order to remove the excess of free dye by gel filtration. The CpfC:dansyl labelling ratio was determined by spectrophotometric quantification of the dye ($\epsilon_{331\text{nm}} = 4,000 \text{ M}^{-1} \text{ cm}^{-1}$) (Gustiananda *et al.*, 2004) and of CpfC ($\epsilon_{280\text{nm}} = 47,700 \text{ M}^{-1} \text{ cm}^{-1}$) (Gasteiger *et al.*, 2005), and estimated to be 0.97.

578 **Pull down assays**

Interaction of CpfC and Isds proteins was investigated by pull-down assays. For this purpose, recombinant N-terminal polyhistidine tagged-CpfC was expressed from pET-23b plasmid and purified as described in the previous section. In order to immobilize the overproduced His-tagged-CpfC, 14 mg of protein was loaded onto a Ni-Sepharose fast flow column (GE Healthcare). The column was next washed with 10 mM Tris-HCl, pH 8.0 containing several concentrations of imidazole, and the His-tagged CpfC was eluted at 60 mM imidazole.

In parallel, *E. coli* BL21(DE3)Gold supernatants expressing non-His tagged versions of *S. aureus* IsdG and IsdI (pET-23b) were prepared, separately, as described above. The supernatants were loaded into the CpfC-bound Ni-Sepharose chelating column and washed with buffer 10 mM Tris-HCl, pH 8.0, and proteins that were subsequently eluted with 60 mM imidazole were analysed by SDS-PAGE. To discard non-specific interactions, control experiments were done similarly using the same supernatants loaded into columns with no bounded CpfC-His protein.

591

592

593 **Steady-state fluorescence anisotropy measurements**

Dansyl-labeled CpfC (0.67 μ M) was incubated with variable concentrations of IsdG or IsdI in buffer A.

The steady-state fluorescence anisotropy of each sample, $\langle r \rangle$, was calculated according to:

$$\langle r \rangle = \frac{I_{VV} - G \cdot I_{VH}}{I_{VV} + 2 G \cdot I_{VH}} \quad (1)$$

where I_{VV} and I_{VH} are the fluorescence intensities (blank subtracted) of the vertically and horizontally polarized emission, when the sample is excited with vertically polarized light, respectively. The G factor ($G = I_{HV}/I_{HH}$) is an instrument correction factor which takes into account the transmission efficiency of the monochromator to the polarization of the light. Measurements were performed at 25 °C on a Fluorolog-3-21 spectrofluorometer (Horiba Jobin Yvon) with automated dual polarizers using 5-mm path length quartz cuvettes. The excitation wavelength was 340 nm with a bandwidth of 6 nm, and the fluorescence emission was recorded at 530 nm with 5 nm bandwidth. K_d and $\langle r \rangle_b$ parameters were obtained by fitting the experimental data (steady-state fluorescence anisotropy, $\langle r \rangle$ versus $[P2]_t$, the total concentration of the binding partner 2 (dimeric IsdG or IsdI)) using the equation:

$$\langle r \rangle = \langle r \rangle_f + \frac{([P1]_t + [P2]_t + K_d) - \sqrt{([P1]_t + [P2]_t + K_d)^2 - 4[P1]_t[P2]_t} (\langle r \rangle_b - \langle r \rangle_f)}{2[P2]_t}$$

where $[P1]_t$ represents the total concentration of the binding partner 1. The concentration of CpfC was fixed to 0.67 μ M during the non-linear regression and assumed that the fluorescently-labelled protein is monomeric in solution; $[P2]_t$ is the total concentration of the binding partner 2. Binding stoichiometry was considered 1:1; $\langle r \rangle_f$ represents the steady-state fluorescence anisotropy of the free protein. $\langle r \rangle_f = 0.165$ (fixed during the analysis); and $\langle r \rangle_b$ the steady-state fluorescence anisotropy of the bound protein.

Förster Resonance Energy Transfer (FRET) and Fluorescence Lifetime Imaging Microscopy (FLIM)

E. coli BL21(DE3)Gold were co-transformed with plasmids that express combinations of CpfC, ChdC, IsdI and IsdG fused to GFP and mCherry (mCh) fluorophore proteins, namely pBCB-*cpfC-gfp* and pBCB-*isdG-mCh*; pBCB-*cpfC-gfp* and pBCB-*isdI-mCh*; pBCB-*chdC-gfp* and pBCB-*isdG-mCh*; and pBCB-*chdC-gfp* and pBCB-*isdI-mCh* (Supplementary Table 1). Cells grown overnight in LB were sub-cultured into LB medium to an OD₆₀₀ of 0.15, supplemented with 1 mM IPTG and grown for 4 h. Cells (2 ml) were centrifuged at 4300 $\times g$ for 3 min, and fixed by incubation with 4% formaldehyde (vol/vol) in PBS, at room temperature, for 30 min and 90 rpm, washed with PBS and immobilized on 8 well μ -slides (Ibidi, slides, Germany) for FRET-FLIM experiments.

621 All measurements were acquired in a Leica TCS SP5 (Leica Microsystems CMS GmbH, Mannheim,
 622 Germany) inverted confocal microscope (DMI6000). A 63x apochromatic water immersion objective
 623 with a NA of 1.2 (Zeiss, Jena Germany) was used for all experiments. GFP and mCherry were excited
 624 respectively with the 476 nm and 514 nm lines from an Argon laser, and fluorescence emission was
 625 collected in the 485-540 nm range for GFP, and 580-700 nm for mCherry. In these conditions, spectral
 626 bleed-through was negligible.

627 Fluorescence lifetime imaging microscopy (FLIM) measurements were performed by time correlated
 628 single photon counting (TCSPC) using the confocal microscope coupled to a multiphoton Titanium:
 629 Sapphire laser (Spectra-Physics Mai Tai BB, Darmstadt, Germany) as the excitation source. FLIM data
 630 was acquired during 90-180 seconds to achieve reasonable photon statistics. The excitation wavelength
 631 was set to 840 nm and emission light was selected with a dichroic beam splitter with an excitation SP700
 632 short-pass filter and an emission 525±25 nm band-pass filter inserted in front of the photomultiplier.
 633 Images were acquired using a Becker and Hickl SPC 830 module. Fluorescence decays for each cell were
 634 calculated by integrating the FLIM data for all pixels of each individual cell. Fluorescence lifetimes were
 635 obtained by analysing the fluorescence decays through a least square iterative re-convolution of decay
 636 functions with the instrument response function (IRF) using the software SPCImage (Becker and Hickl,
 637 Berlin, Germany). Intensity-weighted mean fluorescence lifetime ($\langle\tau\rangle$) of multiexponential decays were
 638 calculated as $\langle\tau\rangle = \sum_i \alpha_i \tau_i$, where α_i are the pre-exponential factors and τ_i are the individual lifetime
 639 values. Average FRET efficiencies in each cell can be determined from $\langle E \rangle = 1 - \langle\tau\rangle_{DA}/\langle\tau\rangle_D$, where $\langle\tau\rangle_{DA}$
 640 and $\langle\tau\rangle_D$ are the donor intensity-weighted mean fluorescence lifetime in the presence or absence of
 641 acceptor, respectively. Assays were done for two independent biological samples and FRET efficiencies
 642 were determined for several cells.

643

644 Genomic analysis

645 A dataset composed of 5060 complete prokaryotic genomes was downloaded from RefSeq (June 2016)
 646 (Pruitt *et al.*, 2004). These correspond to all complete genomes available at the time in RefSeq.
 647 Taxonomic information was retrieved from NCBI and genomes were grouped by phylum or class.
 648 Homologous proteins involved in the several steps of haem biosynthesis and uptake (Urogen III
 649 synthesis: GtrR, GsaM, PbgS, HmbS and UroS; PPD haem biosynthesis UroD-(CgdC/CgdH)-
 650 (PgoX/PgdH1/PgdH2)-PpfC; alternative haem biosynthesis: AhbABCD; *S. aureus* haem biosynthesis
 651 variant: UroD-CgoX-CpfC-ChdC; *Staphylococcus* haem uptake and degradation: HstABC, IsdABCDEFGHI-
 652 SrtB, *B. subtilis* haem uptake: IsdCEDFGX1X2-Hal; haem monooxygenases IsdG-type: MhuD, HmuQ/D;
 653 other haem monooxygenases: HemO, HmuO, HmuS, HugZ, ChuS; haem transporters: HmuTUV, IsdEFD,
 654 HtsABC, Rv2002c-Rv2003-Rv2006c) were identified by BLAST (Altschul *et al.*, 1997) (E-value smaller than
 655 10^{-10} and local amino acid identity of at least 25%). To distinguish between haem transporters systems

656 from siderophores and/or cobalamin importers, sequences from biochemically-characterized
657 transporters were used as queries as well. All query proteins are listed in Supplementary Data 1. When
658 relevant, PFAM-A domain annotations were obtained by using the HMM approach as available at PFAM
659 (Finn *et al.*, 2016). Query coverage, gene fusions and genomic organization were also used for the
660 identification of true positive hits. Due to their small length, to distinguish between the different IsdG
661 homologous, an all versus all blast of putative IsdGs and query sequences and an alignment were
662 performed. Hits were classified according to their best hit based on sequence identity, conservation of
663 the catalytic triad (for HmoA) and sequence length. Selected IsdG-type homologous identified by Blast
664 were aligned with ClustalO (Sievers *et al.*, 2011) and a maximum likelihood tree reconstructed with
665 IQTree (Best-model selection WAG+G4)(Nguyen *et al.*, 2015).

666 To distinguish between “bona fide” CgdH from highly similar non-functional CgdHs, all genomes were
667 also queried for the presence of non-functional CgdH in a similar way as in Dailey *et al* 2015 (Dailey *et*
668 *al.*, 2015). To distinguish between ChdC and chlorite dismutases, sequences were aligned with ClustalO
669 and a phylogenetic tree performed. Sequences corresponding to chlorite dismutases were discarded
670 based on the conservation of the catalytic residues and position within a phylogenetic tree. A haem
671 biosynthesis pathway was only considered to be present in a genome if: 1) 80% of its genes were
672 identified and 2) if the characteristic proteins were present, CgdH and/or CgdC for classical haem
673 pathway and ChdC for *S. aureus* variant. Cases in which a variant of the canonical pathways above
674 described were present and/or missing one gene were assigned as hybrid or incomplete. Due to the high
675 sequence similarity between genes involved in haem d1 biosynthesis with genes from the haem
676 alternative pathway (Bali *et al.*, 2011), in organisms containing *cd*₁ nitrite reductase, the haem
677 alternative pathway identified genes were considered to be involved in haem *d*₁ synthesis instead.

678

679 **Statistical analysis**

680 In all figures, error bars represent the standard deviation of at least two biological samples. Statistical
681 differences were calculated by the two-tailed Student's t-test using GraphPad Prism (GraphPad
682 Software).

683

684

685 **Acknowledgements**

686

687 We are grateful to Mark O'Brian (University of Buffalo), Mariana Pinho (Instituto Tecnologia Química e
688 Biológica António Xavier), and Simon Foster (University of Sheffield) for their generous gift of the Δ *visA*

689 strain, pBCB and pWhiteWalker plamids, respectively. We also thank Patrícia Ferreira for technical
690 support. This work was financially supported by: Project LISBOA-01-0145-FEDER-007660 (Microbiologia
691 Molecular, Estrutural e Celular) funded by FEDER funds through COMPETE2020 - Programa Operacional
692 Competitividade e Internacionalização (POCI) and by national funds through FCT - Fundação para a
693 Ciência e a Tecnologia" for grants PTDC/BBB-BQB/5069/2014, SFRH/BD/95912/2013 (MAMV) and
694 SFRH/BD/118545/2016 (LSOS).
695
696
697
698

699 **References**

- 700 Altschul, S.F., Madden, T.L., Schäffer, A.A., Zhang, J., Zhang, Z., Miller, W., and Lipman, D.J. (1997)
 701 Gapped BLAST and PSI-BLAST: a new generation of protein database search programs. *Nucleic Acids Res*
 702 **25**: 3389–402.
- 703 Anzaldi, L.L., and Skaar, E.P. (2010) Overcoming the heme paradox: heme toxicity and tolerance in
 704 bacterial pathogens. *Infect Immun* **78**: 4977–4989.
- 705 Bali, S., Lawrence, A.D., Lobo, S.A., Saraiva, L.M., Golding, B.T., Palmer, D.J., *et al.* (2011) Molecular
 706 hijacking of siroheme for the synthesis of heme and *d1* heme. *Proc Natl Acad Sci U S A* **108**: 18260–5.
- 707 Bibb, L.A., Kunkle, C.A., and Schmitt, M.P. (2007) The ChrA-ChrS and HrrA-HrrS signal transduction
 708 systems are required for activation of the *hmuO* promoter and repression of the *hemA* promoter in
 709 *Corynebacterium diphtheriae*. *Infect Immun* **75**: 2421–2431.
- 710 Brooijmans, R., Smit, B., Santos, F., Riel, J. van, Vos, W.M. de, and Hugenholtz, J. (2009) Heme and
 711 menaquinone induced electron transport in lactic acid bacteria. *Microb Cell Fact* **8**: 28.
- 712 Choby, J.E., and Skaar, E.P. (2016) Heme synthesis and acquisition in bacterial pathogens. *J Mol Biol* 16–
 713 18.
- 714 Dailey, H.A., Dailey, T.A., Gerdes, S., Jahn, D., Jahn, M., O'Brian, M.R., and Warren, M.J. (2017)
 715 Prokaryotic heme biosynthesis: multiple pathways to a common essential product. *Microbiol Mol Biol*
 716 *Rev* **81**: e00048-16.
- 717 Dailey, H.A., Gerdes, S., Dailey, T.A., Burch, J.S., and Phillips, J.D. (2015) Noncanonical coproporphyrin-
 718 dependent bacterial heme biosynthesis pathway that does not use protoporphyrin. *Proc Natl Acad Sci U*
 719 *S A* **112**: 2210–5.
- 720 Finn, R.D., Coghill, P., Eberhardt, R.Y., Eddy, S.R., Mistry, J., Mitchell, A.L., *et al.* (2016) The Pfam protein
 721 families database: towards a more sustainable future. *Nucleic Acids Res* **44**: D279-85.
- 722 Frustaci, J.M., and O'Brian, M.R. (1993) The *Escherichia coli* *visA* gene encodes ferrochelatase, the final
 723 enzyme of the heme biosynthetic pathway. *J Bacteriol* **175**: 2154–2156.
- 724 Gasteiger, E., Hoogland, C., Gattiker, A., Duvaud, S., Wilkins, M.R., Appel, R.D., and Bairoch, A. (2005)
 725 Protein Identification and Analysis Tools on the ExPASy Server. In *The Proteomics Protocols Handbook*.
 726 pp. 571–607.
- 727 Gustiananda, M., Liggins, J.R., Cummins, P.L., and Gready, J.E. (2004) Conformation of prion protein
 728 repeat peptides probed by FRET measurements and molecular dynamics simulations. *Biophys J* **86**: 2467–
 729 2483.
- 730 Hammer, N.D., Cassat, J.E., Noto, M.J., Lojek, L.J., Chadha, A.D., Schmitz, J.E., *et al.* (2014) Inter- and
 731 intraspecies metabolite exchange promotes virulence of antibiotic-resistant *Staphylococcus aureus*. *Cell*
 732 *Host Microbe* **16**: 531–537.
- 733 Hammer, N.D., Reniere, M.L., Cassat, J.E., Zhang, Y., Hirsch, A.O., Hood, M.I., and Skaar, E.P. (2013) Two
 734 heme-dependent terminal oxidases power *Staphylococcus aureus* organ-specific colonization of the
 735 vertebrate host. *MBio* **4**: 1–9.
- 736 Heinemann, I.U., Jahn, M., and Jahn, D. (2008) The biochemistry of heme biosynthesis. *Arch Biochem*

- 737 *Biophys* **474**: 238–251.
- 738 Jameson, D.M., and Ross, J.A. (2010) Fluorescence Polarization/Anisotropy in Diagnostics and Imaging.
- 739 *Chem Rev* **110**: 2685–2708.
- 740 Levicán, G., Katz, A., Armas, M. de, Núñez, H., and Orellana, O. (2007) Regulation of a glutamyl-tRNA
- 741 synthetase by the heme status. *Proc Natl Acad Sci U S A* **104**: 3135–3140.
- 742 Lobo, S.A.L., Scott, A., Videira, M.A.M., Winpenny, D., Gardner, M., Palmer, M.J., *et al.* (2015)
- 743 *Staphylococcus aureus* haem biosynthesis: characterisation of the enzymes involved in final steps of the
- 744 pathway. *Mol Microbiol* **97**: 472–487.
- 745 Lobo, S.A.L., Warren, M.J., and Saraiva, L.M. (2012) Sulfate-reducing bacteria reveal a new branch of
- 746 tetrapyrrole metabolism. *Adv Microb Physiol* **61**: 267–295.
- 747 Mayfield, J. a., Hammer, N.D., Kurker, R.C., Chen, T.K., Ojha, S., Skaar, E.P., and DuBois, J.L. (2013) The
- 748 chlorite dismutase (HemQ) from *Staphylococcus aureus* has a redox-sensitive heme and is associated
- 749 with the small colony variant phenotype. *J Biol Chem* **288**: 23488–23504.
- 750 Mazmanian, S.K., Skaar, E.P., Gaspar, A.H., Humayun, M., Gornicki, P., Jelenska, J., *et al.* (2003) Passage
- 751 of heme-iron across the envelope of *Staphylococcus aureus*. *Science* **299**: 906–9.
- 752 McGoldrick, H.M., Roessner, C.A., Raux, E., Lawrence, A.D., McLean, K.J., Munro, A.W., *et al.* (2005)
- 753 Identification and characterization of a novel vitamin B12 (cobalamin) biosynthetic enzyme (CobZ) from
- 754 *Rhodobacter capsulatus*, containing flavin, heme, and Fe-S cofactors. *J Biol Chem* **280**: 1086–1094.
- 755 McNicholas, P.M., Javor, G., Darie, S., and Gunsalus, R.P. (1997) Expression of the heme biosynthetic
- 756 pathway genes *hemCD*, *hemH*, *hemM* and *hemA* of *Escherichia coli*. *FEMS Microbiol Lett* **146**: 143–148.
- 757 Nguyen, L.T., Schmidt, H.A., Haeseler, A. Von, and Minh, B.Q. (2015) IQ-TREE: A fast and effective
- 758 stochastic algorithm for estimating maximum-likelihood phylogenies. *Mol Biol Evol* **32**: 268–274.
- 759 Pruitt, K.D., Tatusova, T., and Maglott, D.R. (2004) NCBI Reference Sequence (RefSeq): a curated non-redundant
- 760 sequence database of genomes, transcripts and proteins. *Nucleic Acids Res* **33**: D501–D504.
- 761 Reniere, M.L., Haley, K.P., and Skaar, E.P. (2011) The flexible loop of *Staphylococcus aureus* IsdG is required for its
- 762 degradation in the absence of heme. *Biochemistry* **50**: 6730–7.
- 763 Reniere, M.L., and Skaar, E.P. (2008) *Staphylococcus aureus* haem oxygenases are differentially regulated
- 764 by iron and haem. *Mol Microbiol* **69**: 1304–1315.
- 765 Reniere, M.L., Ukpabi, G.N., Harry, S.R., Stec, D.F., Krull, R., Wright, D.W., *et al.* (2010) The IsdG-family of
- 766 haem oxygenases degrades haem to a novel chromophore. *Mol Microbiol* **75**: 1529–1538.
- 767 Sievers, F., Wilm, A., Dineen, D., Gibson, T.J., Karplus, K., Li, W., *et al.* (2011) Fast, scalable generation of
- 768 high-quality protein multiple sequence alignments using Clustal Omega. *Mol Syst Biol* **7**: 539.
- 769 Skaar, E.P., Gaspar, A.H., and Schneewind, O. (2004) IsdG and IsdI, heme-degrading enzymes in the
- 770 cytoplasm of *Staphylococcus aureus*. *J Biol Chem* **279**: 436–443.
- 771 Skaar, E.P., and Schneewind, O. (2004) Iron-regulated surface determinants (Isd) of *Staphylococcus*
- 772 *aureus*: Stealing iron from heme. *Microbes Infect* **6**: 390–397.
- 773 Skaar EP, Humayun M, Bae T, DeBord KL, S.O. (2004) Iron-source preference of *Staphylococcus aureus*
- 774 infections. *Science* **305**: 1626–8.

- 775 Sousa, F.L., Thiergart, T., Landan, G., Nelson-Sathi, S., Pereira, I.A.C., Allen, J.F., *et al.* (2013) Early
776 bioenergetic evolution. *Philos Trans R Soc B Biol Sci* **368**: 20130088–20130088.
- 777 Stauff, D.L., Bagaley, D., Torres, V.J., Joyce, R., Anderson, K.L., Kuechenmeister, L., *et al.* (2008)
778 *Staphylococcus aureus* HrtA Is an ATPase required for protection against heme toxicity and prevention
779 of a transcriptional heme stress response. *J Bacteriol* **190**: 3588–3596.
- 780 Tarai, B., Das, P., and Kumar, D. (2013) Recurrent challenges for clinicians: emergence of methicillin-
781 resistant *Staphylococcus aureus*, vancomycin resistance, and current treatment options. *J Lab Physicians*
782 **5**: 71.
- 783 Thöny-Meyer, L. (1997) Biogenesis of respiratory cytochromes in bacteria. *Microbiol Mol Biol Rev* **61**:
784 337–76.
- 785 Torres, V.J., Stauff, D.L., Pishchany, G., Bezbradica, J.S., Gordy, L.E., Iturregui, J., *et al.* (2007) A
786 *Staphylococcus aureus* regulatory system that responds to host heme and modulates virulence. *Cell Host*
787 *Microbe* **1**: 109–19.
- 788 Valeur, B., and Berberan-Santos, M.N. (2012) *Molecular Fluorescence: Principles and Applications*,
789 *Second Edition*. .
- 790 Wang, L.Y., Brown, L., Elliott, M., and Elliott, T. (1997) Regulation of heme biosynthesis in *Salmonella*
791 *typhimurium*: Activity of glutamyl-tRNA reductase (HemA) is greatly elevated during heme limitation by
792 a mechanism which increases abundance of the protein. *J Bacteriol* **179**: 2907–2914.
- 793 Wolf, H., Lang, W., and Zander, R. (1984) Alkaline haematin D-575, a new tool for the determination of
794 haemoglobin as an alternative to the cyanhaemoglobin method. I. Description of the method. *Clin Chim*
795 *Acta* **136**: 95–104.

796

797

798

799

800

801

802

803

804

805

806

807

808

809

810

811

812

813

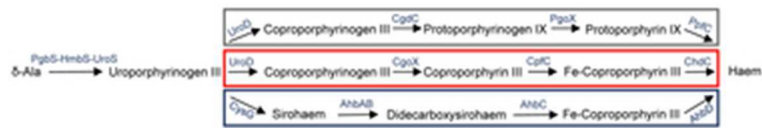


Figure 1. Three different haem biosynthesis pathways that diverge from uroporphyrin III. The enzymes in the three pathways are conserved between aminolaevulinic acid (δ -Ala) and uroporphyrinogen III. The protoporphyrin dependent (or classical) pathway is boxed in grey and converts uroporphyrinogen III into haem using protoporphyrin as an intermediate. The CPD pathway is represented in red and the sirohaem dependent pathway (alternative haem biosynthesis pathway) highlighted in blue.

32x5mm (300 x 300 DPI)

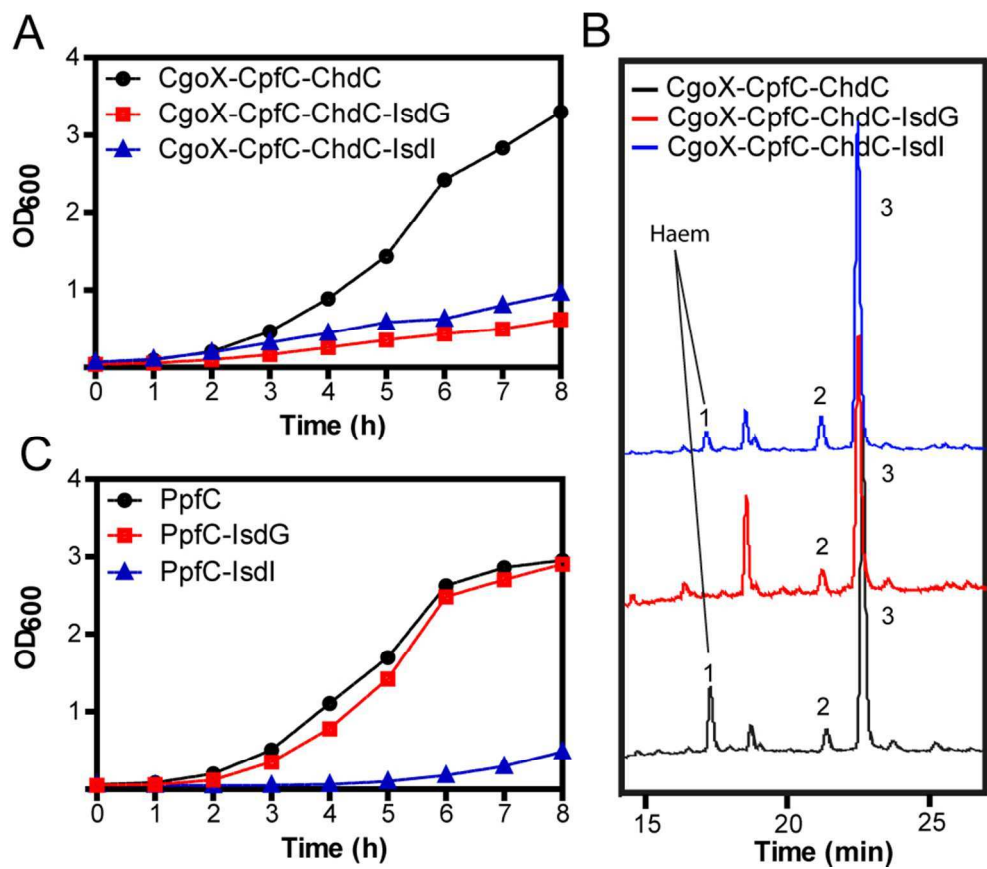


Figure 2. *S. aureus* IsdG and IsdI impair haem formation. (A) Growth of *E. coli* ΔppfC cells complemented with *S. aureus* CgoX-CpfC-ChdC alone, in the presence of *S. aureus* IsdG (CgoX-CpfC-ChdC-IsdG) or *S. aureus* IsdI (CgoX-CpfC-ChdC-IsdI). (B) HPLC-MS profile of cells depicted in (A), with peaks corresponding to haem ($m/z = 616$; peak 1), iron-coproporphyrin III ($m/z = 708$; peak 2), and protoporphyrin IX ($m/z = 553$; peak 3). (C) Growth of *E. coli* ΔppfC cells complemented with *E. coli* PpfC alone and together with *S. aureus* IsdG (PpfC-IsdG) or *S. aureus* IsdI (PpfC-IsdI). Experiments were performed for two independent biological samples.

86x74mm (300 x 300 DPI)

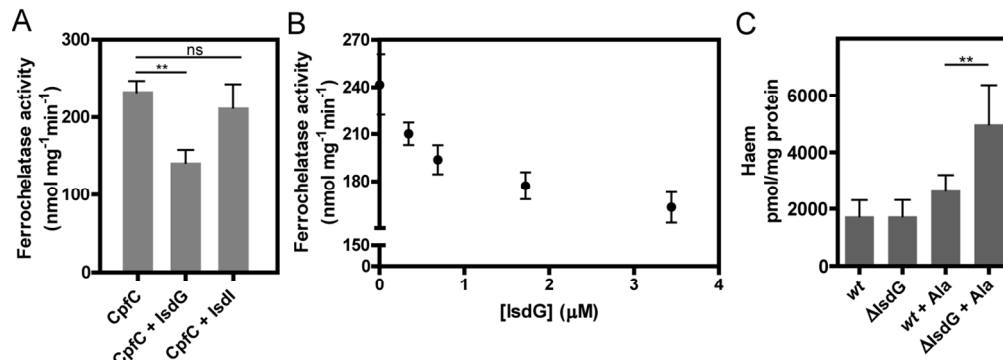


Figure 3. Influence of *S. aureus* IsdG on the CPD pathway. (A) IsdG decreases the ferrochelatase activity of *S. aureus* CpfC while IsdI does not impair the activity. (B) Inhibition of *S. aureus* CpfC ferrochelatase activity increases with IsdG concentration. (C) Intracellular haem quantification of *S. aureus* wild type and Δ IsdG mutant for cells grown in the presence of 400 μ M of aminolaevulinic acid (Ala).

In (A) and (B), activities were measured in reaction mixtures containing CpfC alone, or with the addition of IsdG or IsdI, using coproporphyrin III (10 μ M) and (NH₄)₂Fe(SO₄)₂ (10 μ M) as substrates. In (B), IsdG was used in the following concentrations: 0.3, 0.7, 1.7 and 3.4 μ M. Data depict the mean and standard deviation of three samples using a two-tailed unpaired Student's t-test (** $p < 0.01$).

123x45mm (300 x 300 DPI)

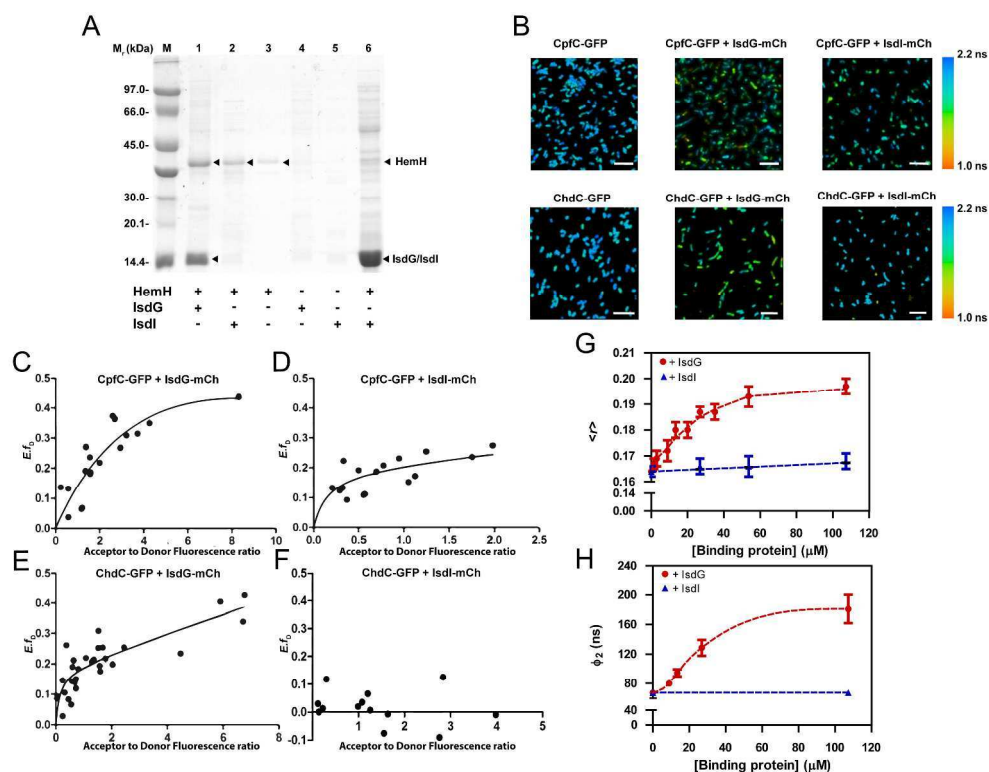


Figure 4. *S. aureus* CpfC and IsdG interact in vivo. (A) Ni-Sepharose pull down assays using CpfC-His tagged protein. Supernatants of *E. coli* expressing, separately, IsdG and IsdI proteins were loaded into CpfC-His bound or unbound columns and pulled down with imidazole. Figure depicts the protein molecular mass marker (M), protein fractions eluted at 60 mM imidazole (lanes 1 to 5), and protein fraction eluted with 10 mM Tris-HCl pH 8.0 following load with IsdI expressing supernatant into a CpfC-His tag bound column (lane 6). (B) Representative FLIM-FRET data of *E. coli* cells co-expressing CpfC-GFP or ChdC-GFP with IsdG-mCherry or IsdI-mCherry, shown as false colour lifetime images. Average fluorescence lifetime ($\langle\tau\rangle$) was rendered as colour according to the colour index indicated on the right. Scale bar represents 10 μ m. For each cell in (B), the calculated average FRET efficiency (E) is plotted against the ratio of fluorescence (as measured by confocal microscopy) from the acceptor (mCherry) construct over donor (GFP), for CpfC-GFP/IsdG-mCherry (C), CpfC-GFP/IsdI-mCherry (D), ChdC-GFP/IsdG-mCherry (E), and ChdC-GFP/IsdI-mCherry (F). Lines are drawn as a guide to the eye. Data are from one representative sample. (G) Steady-state and (H) time-resolved fluorescence polarization binding assay between dansylated CpfC and IsdG or IsdI. (G) The steady-state fluorescence anisotropy, $\langle r \rangle$, and (H) long rotational correlation time, ϕ_2 , of dansylated CpfC are plotted as a function of IsdG (red circles) and IsdI (blue triangles) concentrations expressed as monomers. Conditions consisted of 0.7 μ M dansyl-labeled CpfC in 50 mM Tris-HCl buffer pH 8.0, at 25 $^{\circ}$ C. Dansyl fluorescence was monitored at 530 nm with excitation at 340 nm. The cuvette path length was 5 mm. Data represent the mean values of three independent measurements and error bars represent the standard deviation.

273x210mm (300 x 300 DPI)

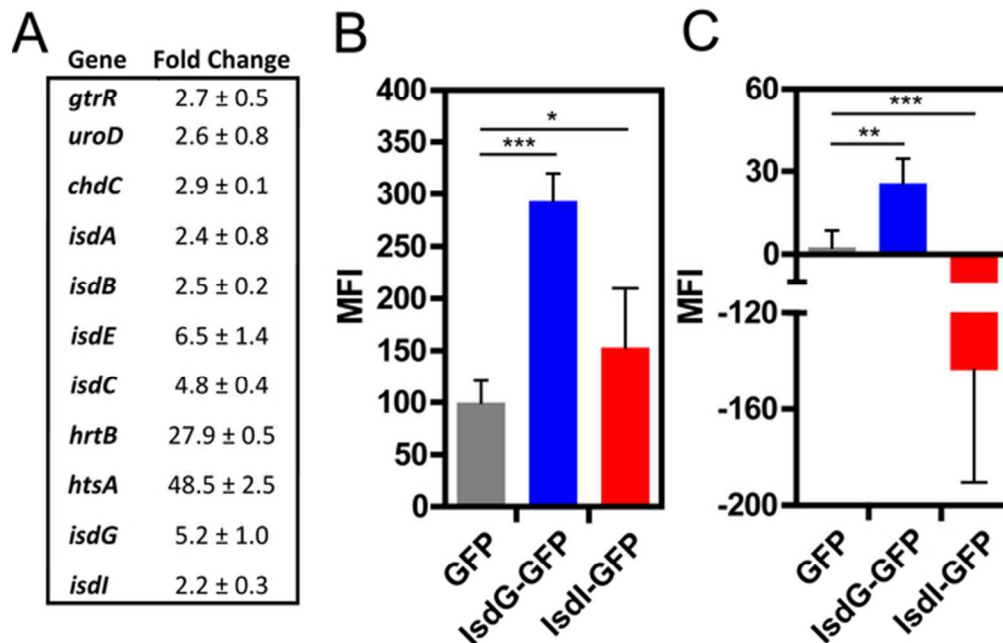
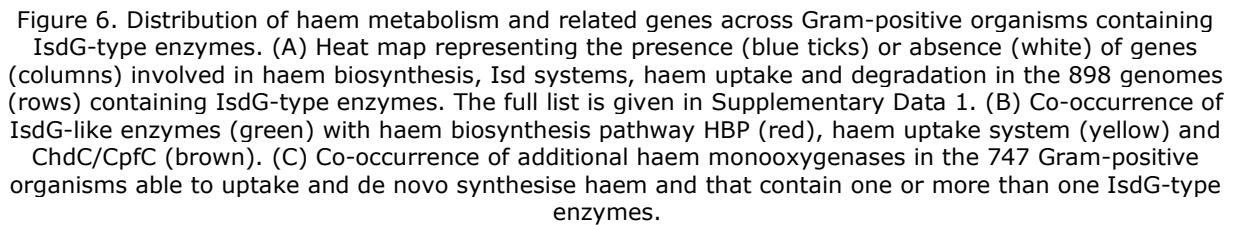


Figure 5. The cellular content of IsdG in *S. aureus* increases upon incubation with haemin. (A) Fold change in abundance of genes coding for enzymes involved in the haem biosynthesis and uptake pathways upon exposure to haemin. (B) Difference of the median GFP fluorescence intensity (MFI) between haemin-treated (5 μ M) and untreated cells. (C) Difference of the median GFP fluorescence intensity between aminolaevulinic acid -treated (400 μ M) and untreated cells. Fluorescence was measured in a flow cytometer and over 300,000 cells were counted. Data represent the mean and standard deviation of four measurements, using the two-tailed unpaired Student's t-test (** $p < 0.001$, ** $p=0.005$ * $p=0.04$).

56x36mm (300 x 300 DPI)



148x108mm (300 x 300 DPI)

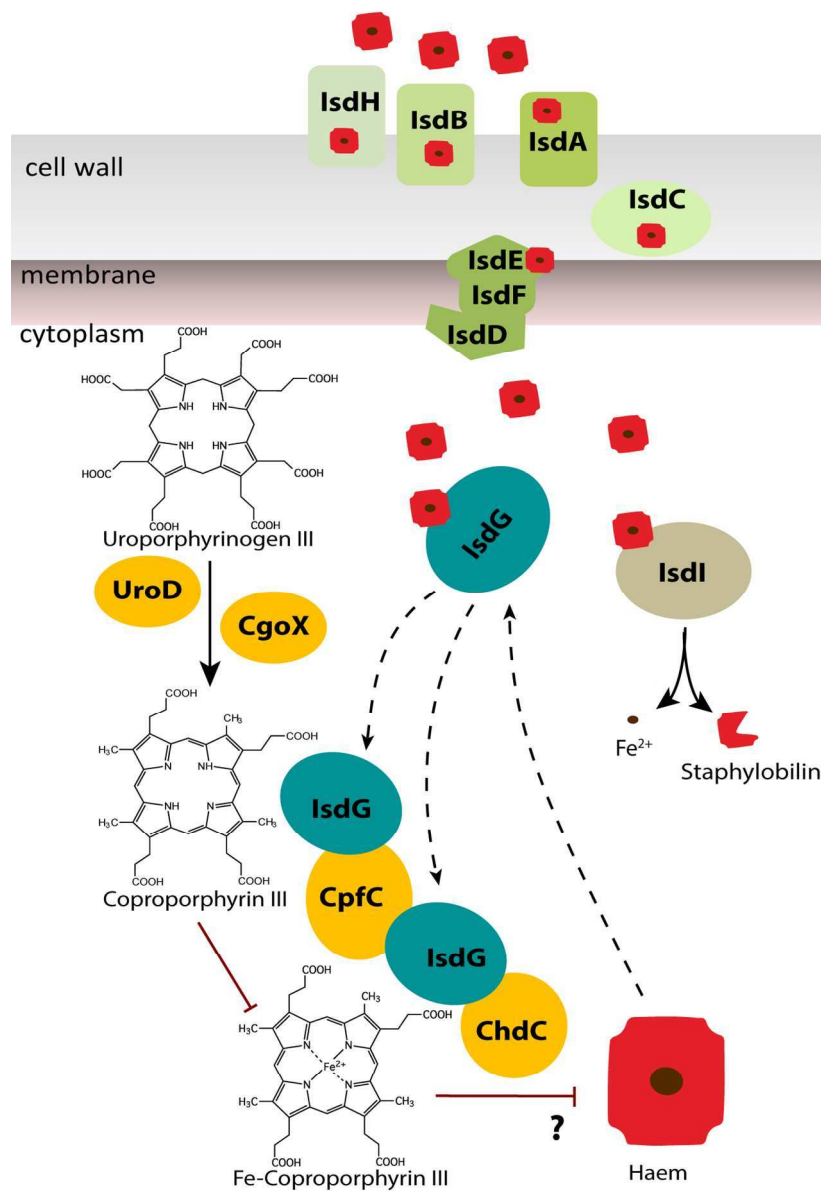


Figure 7. Proposed scheme for the role of IsdG-like proteins in the control of haem production through crosstalk between haem biosynthesis and uptake systems. *S. aureus* CPD is represented proceeding from uroporphyrinogen III to haem via the UroD, CgoX, CpfC and ChdC enzymes. *S. aureus* haem uptake is represented by the Isd system. In this scheme, IsdH and IsdB scavenge haemoglobin haem which enters into the cell through IsdA, IsdC and IsdEFD. In the cytoplasm, haem is mainly degraded by IsdI to staphylobilin, iron and formaldehyde. Increase of haem content augments the IsdG abundance to levels that allow its interaction with CpfC, resulting in the inhibition of the CPD pathway.

111x163mm (300 x 300 DPI)